International Journal of Applied Electromagnetics and Mechanics 65 (2021) 235–251
DOI 10.3233/JAE-190101
IOS Press

Dual solutions for boundary layer flow and heat transfer of biomagnetic fluid over a stretching/shrinking sheet in presence of a magnetic dipole and a prescribed heat flux

Mohammad Ferdows[a,b,*], Md Ghulam Murtaza[b], Jagadis Chandra Misra[c], Efstratios Em Tzirtzilakis[d] and Faris Alzahrani[a]
[a]*Department of Mathematics, Faculty of Science, King Abdulaziz University, Jeddah, Saudi Arabia*
[b]*Research Group of Fluid Flow Modeling and Simulation, Department of Applied Mathematics, University of Dhaka, Dhaka, Bangladesh*
[c]*Centre for Healthcare Science and Technology, Indian Institute of Engineering Science and Technology, Shibpur, Howrah, India*
[d]*Department of Mechanical Engineering, University of the Peloponnese, Trípoli, Greece*

Abstract. This paper analyzes the steady boundary layer flow and heat transfer of biomagnetic fluid over a stretching/shrinking sheet with prescribed surface heat flux under the influence of a magnetic dipole. The governing equations are transformed into a set of ordinary differential equations (ODEs) by using similarity transformations. Numerical results are obtained using the boundary value problem solver bvp4c of MATLAB. The effects of various physical parameters on the velocity and temperature profiles as well as skin friction coefficient are discussed. The paper shows that dual solutions exist for certain values of stretching/shrinking sheet and suction parameters. Stability analysis is performed to determine which solution is stable and physically valid. Results of the stability analysis depict that the first solution (upper branch) is stable and physically realizable, while the second solution (lower branch) is unstable.

Keywords: Biomagnetic fluid, heat transfer, magnetic dipole, stretching/shrinking sheet, dual solutions, stability analysis

1. Introduction

Biomagnetic fluid dynamics (BFD) is a relatively new area in fluid mechanics investigating the fluid dynamics of biological fluids in the presence of a magnetic field. Studies of BFD problems have been receiving growing attention of researchers owing to their potential applications in bioengineering and medical sciences. These include development of various magnetic devices for cell separation, high-gradient magnetic separation, reduction of bleeding during surgeries, targeted transport of drugs using magnetic particles as drug carriers, magnetic resonance imaging of specific parts of the body using strong magnetic fields and treatment of cancer/tumor by using magnetic hyperthermia [1–5].

*Corresponding author: Mohammad Ferdows, Department of Mathematics, Faculty of Science, King Abdulaziz University, P.O. Box 80203, Jeddah 21589, Saudi Arabia; Research group of Fluid Flow Modeling and Simulation, Department of Applied Mathematics, University of Dhaka, Dhaka-100, Bangladesh. E-mail: ferdows@du.ac.bd.

Biomagnetic fluid dynamics model was first developed by Haik et al. [6], using the principles of FHD. Some modifications of the model proposed in [6] were later made by Tzirtzilakis [7]. This model is consistent with the principles of ferrohydrodynamics (FHD) and the magnetohydrodynamics (MHD). Tzirtzilakis and Kafoussias [8] studied the flow of a heated ferrofluid over a linearly stretching sheet under the action of a magnetic field, which is generated by a magnetic dipole. Tzirtzilakis and Tanoudis [9] presented a numerical method for the study of two-dimensional laminar incompressible flow and heat transfer of a biological fluid over a stretching sheet. Misra and Shit [10,11] investigated flows of biomagnetic viscoelastic fluids in different situations and made an important observation that the presence of an external magnetic field influences the flow of biomagnetic fluids quite significantly. The problem of biomagnetic fluid flow under the influence of a spatially varying magnetic field was studied by Nor Amirah Idris et al. [12].

Recently, Murtaza et al. [13] investigated the combined effect of electrical conductivity and magnetization on biomagnetic fluid flow over a stretching sheet. Reddy et al. [14] analyzed the magnetohydrodynamic flow of blood in a permeable inclined stretching surface in the presence of an external magnetic field with heat and mass transfer. Siddiqa et al. [15] investigated the effects of thermal radiation and magnetic field on two dimensional biomagnetic fluid flows. This study was motivated towards studying the behavior of blood flow and heat transfer in the presence of a magnetic field combined with thermal radiation effects. Sushma et al. [16] studied the slip flow effect of MHD blood flow in the presence of heat source/sink and chemical reaction and reported that blood velocity near the vessel wall reduces as the slip parameter is increased.

Mukhopadhyay [17] studied the effect of heat transfer on the flow of a moving fluid on a moving flat surface and observed the existence of dual solutions. Naganthran et al. [18] studied the flow and heat transfer of a third grade fluid and also found dual solutions for the flow field. Krishna et al. [19] reported that dual solutions exist for the unsteady flow of a fluid flowing over an inclined stretching sheet. Naganthran and Nazar [20] studied the MHD stagnation-point flow and heat transfer over a Stretching/Shrinking Sheet and also found dual solutions existence. Hafidzuddin et al. [21] observed dual solutions for the boundary layer flow and heat transfer with slip velocity over an exponentially stretching/shrinking sheet. Analyses of stable and unstable solutions (dual solutions) and stability were also carried out in a variety of studies by Ghosh et al. [22], Yasin et al. [23], Awaludin [24], Mishra and Singh [25] and Bhattacharyya [26].

Two-dimensional MHD flow of a viscous nanofluid over a nonlinear stretching surface with slip effects of the velocity, temperature and concentration was studied by Hayat et al. [27]. Bovan et al. [28] dealt with a problem of nanofluid flow around a triangular obstacle and observed that the Nusselt number is more sensitive to the Stuart number rather than the orientations of the obstacle and the volumetric concentration of nanoparticles. Das et al. studied the unsteady MHD flow of nanofluids over an accelerating, convectively heated stretching sheet, in the presence of a transverse magnetic field with heat source/sink [29]. Rashidi et al. [30,31] investigated the convective heat transfer of Al_2O_3–water nanofluid over an equilateral triangular obstacle. They performed an optimization analysis and determined the conditions for maximum heat transfer rate and minimum drag coefficient. Shirejini [32] analyzed nanofluid flow and forced convection in a rotating circular cylinder and reported that the rotation of the cylinder causes reduction in the heat transfer rate. Simulation of the nanofluid flow field and heat transfer in a rotating cylinder was performed by Shima et al. [33]. A comprehensive review on applications of MHD flows in medical and biological sciences was performed by Rashidi et al. [34], who made an observation that during surgery, both blood flow and tissue temperature can be reduced by applying an external magnetic field. Very recently, Misra et al. [46] investigated the effects of heat transfer and entropy generation on the electrokinetic flow of a nanofluid in a porous microfluidic tube. The results of the study bear the promise of important applications in biomedical engineering.

Results of studies on three-dimensional/two-dimensional MHD flows were reported in [35,36] , which were conducted by considering the effects of velocity and thermal slip boundary conditions, and the effects of the induced magnetic field. Ahmed et al. [37] investigated combined effects of internal heat generation and mass transfer effects with convective boundary conditions on Casson fluid flow over a linear stretching sheet. The natural convection of laminar flows in enclosures under the influence of a magnetic field was examined by Jalil and Al-Tae'y [38]. In a review article, nanoparticles-based magnetic separation method was discussed by Wang et al. [39].

The effects of the magnetic field on the control of wake structure and vortex shedding behind the obstacles were investigated by Bovan et al. [40]. The analysis was performed for obstacles of different geometrical configurations by using several empirical equations. Values of Stuart numbers were presented for each obstacle. Rashidi and Esfahani [41] analyzed the forced convective heat transfer in a channel with a built-in square obstacle under the action of an external magnetic field. The effects of magnetic field strength and spacing ratios on the drag and lift coeffcients, streamlines and vorticity contours were also examined by Rashidi et al. [42].

Although biomagnetic fluids have important applications in biomedical engineering, none of the studies mentioned above was performed under the purview of biomagnetic fluid dynamics. The possibility of the existence of dual solutions has also not been discussed in those studies. In view of this, the present study has been aimed at investigating the effects of the magnetic parameter and suction parameter on the flow and heat transfer of a biomagnetic fluid over a stretching/shrinking sheet with prescribed heat flux. This study has been conducted, by considering the governing equations of biomagnetic fluid flows. The computational results have been obtained using the built-in bvp4c function in MATLAB. The results of the study reveal that there exist dual solutions for some specific values of suction parameter, stretching parameter and ferromagnetic parameter. Stability analysis has also been carried out, based on which an attempt has been made to determine which solution is stable and physically realistic. The validity of the numerical results presented, has also been established.

2. Mathematical modelling and the governing equations

Let us consider the two-dimensional incompressible boundary layer flow and heat transfer of a biomagnetic fluid over a stretching/shrinking sheet as illustrated in Fig. 1, where x and y are Cartesian coordinates measured along the sheet and normal to it. It is assumed that the free stream velocity is $U_\infty(x) = bx$ and the sheet is stretched or shrunk with the velocity $U_w(x) = ax$, where $a > 0$ implies the stretching situation and $a < 0$ indicates the shrinking condition and b as a positive constant. A magnetic dipole is located below the sheet, at a distance d, i.e. at the point $(0, d)$, $d < 0$, giving rise to a magnetic field of magnetic field strength intensity H. It is assumed that temperature of the sheet is $T_w(x)$, while the ambient temperature is $T_c(x)$ where $T_c(x) > T_w(x)$.

Using boundary layer approximations, the governing equation for the problem can be written as:

$$\frac{\partial u}{\partial x} + \frac{\partial v}{\partial y} = 0 \qquad (1)$$

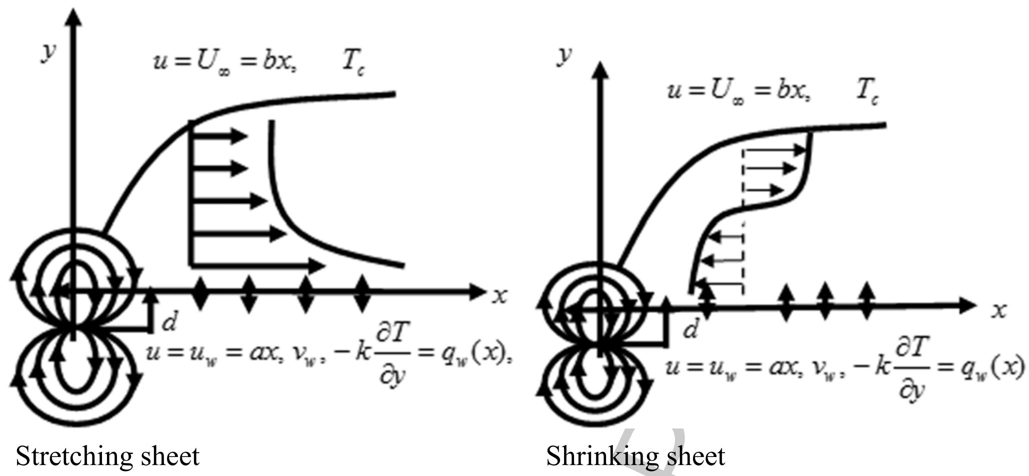

Fig. 1. The geometry of the problem.

$$u\frac{\partial u}{\partial x} + v\frac{\partial u}{\partial y} = U_\infty \frac{\partial U_\infty}{\partial x} + v\frac{\partial^2 u}{\partial y^2} + \frac{\mu_0}{\rho} M \frac{\partial H}{\partial x} \tag{2}$$

$$\rho C_p \left(u\frac{\partial T}{\partial x} + v\frac{\partial T}{\partial y} \right) + \mu_0 T \frac{\partial M}{\partial T} \left(u\frac{\partial H}{\partial x} + v\frac{\partial H}{\partial y} \right) = k\frac{\partial^2 T}{\partial y^2} \tag{3}$$

subject to the boundary conditions

$$\begin{aligned} &u = U_w(x) = ax, \quad v_w(x) = v_w, \quad -k\frac{\partial T}{\partial y} = q_w(x) = -Dx \quad \text{at } y = 0 \\ &u = U_\infty(x) = bx, T \to T_c \quad \text{as } y \to \infty. \end{aligned} \tag{4}$$

where u and v are the velocity components along the x- and y-axes, respectively, ρ is the fluid density, k is the thermal conductivity, c_p is the specific heat at constant pressure, μ is the fluid viscosity, μ_0 is the magnetic permeability and $q_w(x) = -Dx$ is the heat transfer to the wall, D being a positive constant. The above-written governing Eqs (1)–(3) were used in several previous studies (cf. [8,45]). The magnetization parameter M is considered to be related to the temperature T as $M = K\,(T_c - T)$.

The magnetic dipole lies on the y-axis at a distance d below the x-axis, which generates the magnetic field that is sufficiently strong to saturate the biofluid. $H_x,\ H_y$ are the components of the magnetic field $\overrightarrow{H} = (H_x,\ H_y)$ given by

$$H_x(x, y) = -\frac{\gamma}{2\pi}\frac{x^2 - (y+d)^2}{[x^2 + (y+d)^2]^2} \quad \text{and} \quad H_y(x, y) = \frac{\gamma}{2\pi}\frac{2x(y+d)}{[x^2 + (y+d)^2]^2} \quad (cf.\ [13]).$$

The magnitude $\|H\| = H$ of the magnetic field is given by

$$H(x, y) = [H_x^2 + H_y^2]^{1/2} \approx \frac{\gamma}{2\pi}\left[\frac{1}{(y+d)^2} - \frac{1}{2}\frac{x^2}{(y+d)^4}\right]. \tag{5}$$

The mathematical analysis of the problem is simplified by introducing the following dimensionless coordinates [13,44],

$$\xi(x) = \sqrt{\frac{b}{\nu}}x, \quad \eta = \sqrt{\frac{b}{\nu}}y, \quad \psi = \left(\frac{\nu}{\rho}\right)\xi f(\eta), \quad \theta(\eta) = \frac{T_c - T}{T_c - T_w} \tag{6}$$

where $T_c - T_w = \frac{Dx}{k}\sqrt{\frac{\nu}{b}}$ and assumed that temperature of the sheet is $T_w(x)$ while the temperature of the ambient far from the surface of the sheet is $T_c(x)$ [44,45]. Far away from the sheet, the magnetization, $M = K\,(T_c - T)$ is zero and the magnetic field no longer affects the flow field.

We introduce a stream function ψ such that $u = \frac{\partial\psi}{\partial y}$ *and* $v = -\frac{\partial\psi}{\partial x}$ which identically satisfy the continuity Eq. (1).

By substituting (6) and (5) into Eqs (2) and (3), the following similarity equation is obtained for the given problem:

$$f''' + ff'' - f'^2 + 1 - \frac{2\beta\theta}{(\eta+\alpha)^4} = 0 \tag{7}$$

$$\theta'' + P_r f\theta' - \frac{2\lambda_a\beta(\theta-\varepsilon)}{(\eta+\alpha)^3} f = 0. \tag{8}$$

The corresponding transformed boundary conditions are

$$\begin{aligned} &f'(0) = \lambda, \quad f(0) = S, \quad \theta'(0) = -1 \\ &f'(\infty) \to 1, \quad \theta(\infty) \to 0. \end{aligned} \tag{9}$$

The dimensionless parameters, which are of particular interest here are the following:

Prandtl number $P_r = \frac{\mu C_p}{k}$, Ferromagnetic parameter $\beta = \frac{\gamma}{2\pi}\frac{\mu_0 k(T_c - T_w)\rho}{\mu^2}$,

Viscous dissipation parameter $\lambda_a = \frac{c\mu^2}{\rho k(T_c - T_w)}$, Temperature parameter $\varepsilon = \frac{T_c}{(T_c - T_w)}$ and dimensionless distance $\alpha = \sqrt{\frac{c\rho}{\mu}}$. Also $\lambda = \frac{b}{a}$ is the stretching/shrinking parameter/$\lambda > 0$ for a stretching sheet, $\lambda < 0$ represents the case of a shrinking sheet and S is the suction/injection parameter. In the case of suction, $S > 0$ while $S < 0$ indicates injection.

3. Stability analysis

In order to carry out a stability analysis, let us first consider the unsteady case. The Eqs (2) and (3) can be re-written as

$$\frac{\partial u}{\partial t} + u\frac{\partial u}{\partial x} + v\frac{\partial u}{\partial y} = U_\infty\frac{\partial U_\infty}{\partial x} + \nu\frac{\partial^2 u}{\partial y^2} + \frac{\mu_0}{\rho}M\frac{\partial H}{\partial x} \tag{10}$$

$$\frac{\partial T}{\partial t} + \left(u\frac{\partial T}{\partial x} + v\frac{\partial T}{\partial y}\right) + \frac{\mu_0}{\rho C_p}T\frac{\partial M}{\partial T}\left(u\frac{\partial H}{\partial x} + v\frac{\partial H}{\partial y}\right) = \frac{k}{\rho C_p}\frac{\partial^2 T}{\partial y^2} \tag{11}$$

where t denotes time. For the ongoing analysis, the following new dimensionless variables will also be used:

$$u = bx\frac{\partial f}{\partial \eta}(\eta,\tau), v = -\sqrt{b\nu}f(\eta,\tau),$$

$$\eta = \sqrt{\frac{b}{\nu}}y, \quad \tau = bt, \quad \theta(\eta, \tau) = \frac{k(T_c - T)}{Dx}\sqrt{\frac{b}{\nu}}. \tag{12}$$

Using (12), (10) and (11) can be written as

$$\frac{\partial^3 f}{\partial \eta^3} + f\frac{\partial^2 f}{\partial \eta^2} - \left(\frac{\partial f}{\partial \eta}\right)^2 + 1 - \frac{\partial^2 f}{\partial \eta \partial \tau} - \frac{2\beta\theta}{(\eta + \alpha)^4} = 0 \tag{13}$$

$$\frac{\partial^2 \theta}{\partial \eta^2} + P_r\left(f\frac{\partial \theta}{\partial \eta} - \frac{\partial \theta}{\partial \tau}\right) - \frac{2\lambda_a\beta\,(\varepsilon - \theta)\,f}{(\eta + \alpha)^3} = 0 \tag{14}$$

while the boundary conditions now assume the form

$$\begin{aligned} &f(0, \tau) = S, \quad \frac{\partial f}{\partial \eta}(0, \tau) = \lambda, \quad \frac{\partial \theta}{\partial \eta}(0, \tau) = -1 \\ &\frac{\partial f}{\partial \eta}(\eta, \tau) \to 0, \theta(\eta, \tau) \to 0 \quad \text{as } \eta \to \infty. \end{aligned} \tag{15}$$

To test the stability of the steady flow solution, writing $f(\eta) = f_0(\eta)$, $\theta(\eta) = \theta_0(\eta)$, one can write

$$\begin{aligned} f(\eta,\ \tau) &= f_0(\eta) + e^{-\gamma\tau}F(\eta, \tau) \\ \theta(\eta,\ \tau) &= \theta_0(\eta) + e^{-\gamma\tau}G(\eta, \tau) \end{aligned} \tag{16}$$

where γ is an unknown eigenvalue parameter, and $F(\eta, \tau)$ and $G(\eta, \tau)$ are small as compared to $f_0(\eta)$ and $\theta_0(\eta)$. By substituting (16) into Eqs (13) and (14), the following linearized governing equations are obtained:

$$\frac{\partial^3 F}{\partial \eta^3} + f_0\frac{\partial^2 F}{\partial \eta^2} + f_0^{''}F - 2f_0'\frac{\partial F}{\partial \eta} - \frac{\partial^2 F}{\partial \eta \partial \tau} + \gamma\frac{\partial F}{\partial \eta} - \frac{2\beta G_0}{(\eta + \alpha)^4} = 0 \tag{17}$$

$$\frac{\partial^3 G}{\partial \eta^3} + \Pr\left(f_0\frac{\partial G}{\partial \eta} + \gamma G + \theta_0' F\right) - \frac{2\beta\lambda_a\varepsilon F}{(\eta + \alpha)^3} + \frac{2\beta\lambda_a(f_0 G + \theta_0 F)}{(\eta + \alpha)^3} = 0 \tag{18}$$

which are subject to the boundary conditions

$$\begin{aligned} &F_0(0, \tau) = 0, \quad \frac{\partial F}{\partial \eta}(0, \tau) = 0, \quad G(0, \tau) = 0 \\ &\frac{\partial F}{\partial \eta}(\eta, \tau) \to 0, \quad G(\eta, \tau) \to 0 \quad \text{as } \eta \to \infty. \end{aligned} \tag{19}$$

When $\tau = 0$, the solution of the steady state equations (7) and (8) reduces to. $f(\eta) = f_0(\eta)$ and $\theta(\eta) = \theta_0(\eta)$. Hence, $F(\eta) = F_0(\eta)$ and $G(\eta) = G_0(\eta)$ in (17) and (18) identify initial growth or decay of the solution (16). To test our numerical procedure, the following linear eigenvalue problem will be solved:

$$F_0^{'''} + f_0F_0^{''} + f_0^{''}F_0 - 2f_0^{'}F_0^{'} + \gamma F^{'} - \frac{2\beta G_0}{(\eta + \alpha)^4} = 0 \tag{20}$$

$$G_0^{''} + \Pr\left(f_0G_0^{'} + \gamma G_0 + F_0\theta_0^{'}\right) - \frac{2\beta\lambda\varepsilon F_0}{(\eta + \alpha)^3} + \frac{2\beta\lambda\left(f_0G_0 + \theta_0F_0\right)}{(\eta + \alpha)^3} = 0 \tag{21}$$

along with the new boundary conditions:

$$F_0(0) = 0, \quad F_0^{'}(0) = 0, \quad G_0(0) = 0$$

$$F_0^{'}(\eta) \to 0, \quad G_0(\eta) \to 0 \quad \text{as } \eta \to \infty. \tag{22}$$

The smallest eigenvalue γ will determine the stability of the corresponding steady flow solution $f_0(\eta)$ and $\theta_0(\eta)$ for all parameters involved.

Harris et al. [47] suggested relaxing a boundary condition on $F_0(\eta)$ or $G_0(\eta)$ to better find a range of possible eigenvalues. Following this suggestion, it was decided to relax the condition $F_0'(\eta) \to 0$ *as* $\eta \to \infty$. Accordingly solution of the system (20–21) was found, considering the new boundary condition $F_0''(0) = 1$.

4. Numerical method

The systems of nonlinear ordinary differential Eqs (7) and (8) subject to boundary conditions (9) were solved numerically by using the boundary value problem solver, bvp4c function technique in MATLAB. For finding the solution, the prerequisites are: (i) to reduce the system of higher order partial differential equations to a system of system of first order ordinary differential equations by introducing new variables, (ii) to write down the boundary conditions for the new variables, and (iii) to make appropriate initial guesses for the mew variables.

Since the transformed governing equations are of third order, for reducing them into a system of first order ordinary differential equations, some new variables were defined as $f = y_1, f^{'} = y_2, f^{''} = y_3, \theta = y_4, \theta^{'} = y_5$. Thus, the two coupled higher order differential equations and the corresponding boundary conditions were transformed to a system of five first order ODEs along with new boundary conditions. The system of first order ODEs is:

$$\left.\begin{aligned} f' &= y_2 \\ y_2' &= y_3 \\ y_3' &= -y_1 y_3 + y_2^2 - 1 + \frac{2\beta y_4}{(\eta+\alpha)^4} \\ \theta' &= y_5 \\ y_5' &= -\Pr y_1 y_5 - \frac{2\lambda_a \beta(\varepsilon - y_4) y_1}{(\eta+\alpha)^3} \end{aligned}\right\} \tag{23}$$

subject to the initial boundary conditions:

$$y_1(0) = S, \quad y_2(0) = \lambda,\ y_5(0) = -1, \quad y_2(\infty) = 0, \quad y_4(\infty) = 0 \tag{24}$$

(23), and Eq. (24) have been integrated numerically as an initial value problem to a given terminal point. All these simplifications had to be done for using the MATLAB package. This programme is performed with the step size of $\eta = 0.01$ and then solved for the interval of $0 \le \eta \le \eta_\infty$ taking $\eta_\infty = 3$. This value was obtained by using trial and error method.

The numerical procedure of bvp4c followed is as follows:

- Nonlinear PDEs are reduced to 1st order ODEs .
- The solution is returned by bvp4c as a structure called *sol*
- Mesh selection is generated and returned in the field *sol.x*
- Solution can be fetched from array *sol.y* corresponding to *sol.x*
- $y(0)$ was considered as the left boundary, and $y\infty$ as the right boundary.

The algorithm used is sketched in Fig. 2.

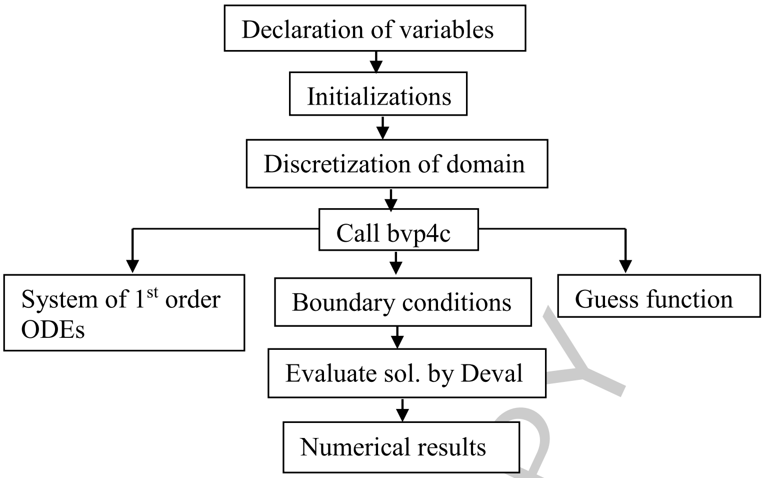

Fig. 2. Algorithm of bvp4c routine in MATLAB.

5. Results and discussion

For the purpose of computation, the fluid is taken to be blood with ρ = 1050 kg/m^3 and $\mu = 3.2 \times 10^{-3}$ kg m^{-1} s^{-1} [13]. The electrical conductivity of blood is σ = 0.8 sm^{-1} [7], T_c = 41 °C and wall temperature T_w = 37 °C. It is known that for temperatures above 41 °C, blood cells may undergo irreversible structural damages and this is the reason why someone's life is in danger if he/she suffers from high fever. This biological limit of 41 °C is the Curie temperature. Beyond this temperature, the magnetization effect on the fluid is not very prominent [7], for the above values of temperature, the temperature is ε = 78.5 and the viscous dissipation number is 6.4×10^{-14} [13]. Generally, the specific heat under a constant pressure c_p and thermal conductivity k of any fluid are temperature- dependent. However, values of dimensionless parameters like the Prandtl number do not change appreciably with the temperature variation. Therefore, for the present study, one can take $c_p = 3.9 \times 10^3$ Jkg^{-1} k^{-1} and k = 0.5 Jm^{-1} s^{-1} k^{-1} and hence P_r = 25 [8,13].

The values of β (which is related to the magnetic field) to be from 0 to 10 (cf. [4]), where $\beta = 0$ corresponds to pure hydrodynamic flow. For the validation of the numerical method, the numerical results for the skin friction coefficient (for a limiting case) are compared with those of Naganthran et al. [43]. The comparative study, presented in Table 1 shows that the results of the present investigation are in good agreement with those reported by Naganthran et al. [43].

The impact of different parameters on the velocity and the temperature profiles are illustrated in Figs 3–12. Different figures also reveal the existence of dual solutions. The figures also show that all the profiles satisfy the far field boundary conditions (9) asymptotically.

Figure 3 illustrates the variation of skin friction coefficient $f''(0)$ with the stretching/shrinking parameter for different values of suction parameter. It is interesting to note that there exist two solutions branches. The first branch represents the stable solution, while the second branch denotes the unstable solution for different values of λ, λ_c which correspond to given values of S. From Fig. 3, it can be observed that a unique solution exists for $\lambda > -0.75$ when $S = 0.5$, $\lambda > -0.9$ and when $S = 0.7$ and $\lambda > -1.1$ when $S = 0.8$, while dual solutions exist for $-1.31 < \lambda < -0.75$ when $S = 0.5$, $-1.595 < \lambda < -0.9$ when $S = 0.7$ and $-1.71 < \lambda < -1.1$. But no solution exists when $\lambda < \lambda_c$ when $\lambda_c = -1.31,\ -1.595, -1.71$ for $S = 0.5$,

Table 1
Comparison of skin friction coefficient for $\beta = 0$, $S = 0$, $Pr = 0.72$

λ	Present		Naganthran et al. [43]		Error in percentage	
	First solution	Second solution	First solution	Second solution	First solution	Second solution
-0.25	1.402239		1.402240		0.0001	-
-0.5	1.49567		1.495669		0.0001	-
-0.75	1.48929		1.489298		0.0008	-
-1.0	1.32882	0.00126	1.328816	0	0.0004	0.126
-1.15	1.08225	0.11576	1.082231	0.116702	0.0019	0.0942
-1.2	0.93253	0.23286	0.932473	0.233649	0.0057	0.0789

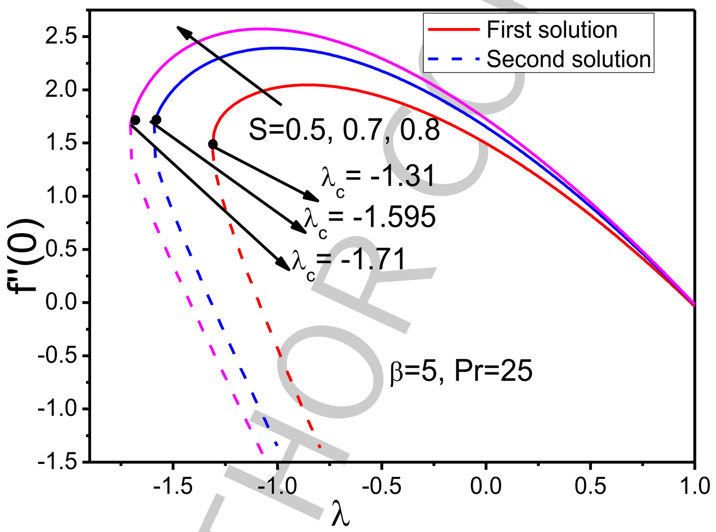

Fig. 3. Variation of skin friction λ for various value of S.

0.7, 0.8, respectively, where λ_c is the critical value of λ at which the two branches of the solution meet each other and thus a unique solution is obtained.

The variation of the skin friction with stretching/shrinking parameter for different values of ferromagnetic number is displayed at Fig. 4. From this figure, it may be observed that the solution is unique when $\lambda > -1.21$; multiple (dual) solutions exist when $\lambda_c < \lambda < -1.21$ and no solution exists when $\lambda < \lambda_c$, where λ_c is the critical value of λ and the value of $\lambda_c = -1.27, -1.31, -1.345$ for $\beta = 1, 5, 10$. From this figure it may be further observed that the critical value λ_c decreases, as the value of the ferromagnetic parameter increases and that of the skin friction decreases. One may note that the effect of the ferromagnetic parameter diminishes in the range of λ for which the solution exists.

Figures 3 and 4 show that increase in the suction parameter results in an increase in the range of λ for which the similarity solution exists. The skin friction at the surface increases as the suction parameter increases. It is also found that the range of λ for which the similarity solution exists is increased, as the ferromagnetic parameter β increases. It may be mentioned that the effect of increasing the suction

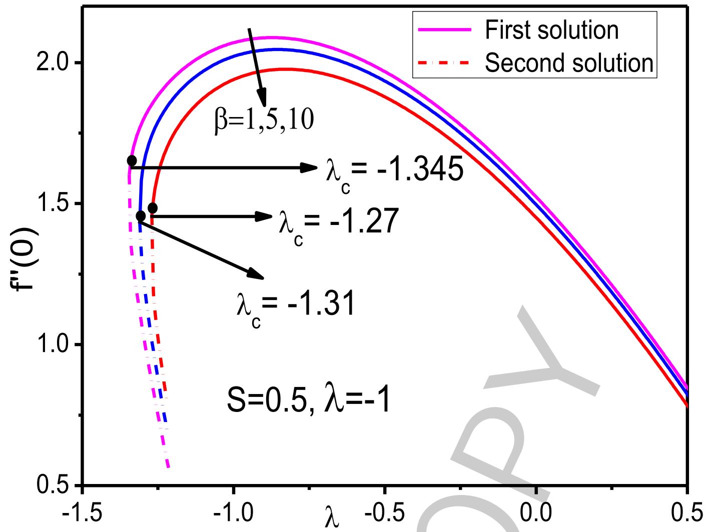

Fig. 4. Variation in skin friction with λ for various values of β.

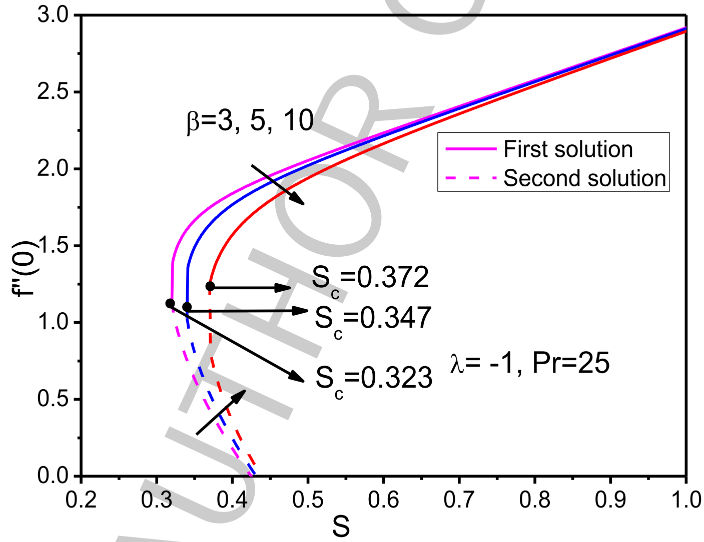

Fig. 5. Variation of skin friction with S for various values of β.

parameter gives rise to an enlargement of the range of λ for which unique solution exists. However, an increase in ferromagnetic parameter gives rise to a reduction in the range of λ for which the unique solution exists.

Figures 5 and 6 show the variation of skin friction coefficient $f''(0)$ with suction parameter S for different values of stretching parameter and ferromagnetic number. It is observed that, dual solutions exist for some specific values of the suction parameter, for different values of ferromagnetic parameter and stretching parameter. Numerically it is seen that for $\beta = 3$, unique solution exists for $S > 0.42$, dual solutions exist for $0.323 < S < 0.42$ and no solutions for $S < 0.323$. For $\beta = 5$, the solution is unique for $S > 0.43$, dual

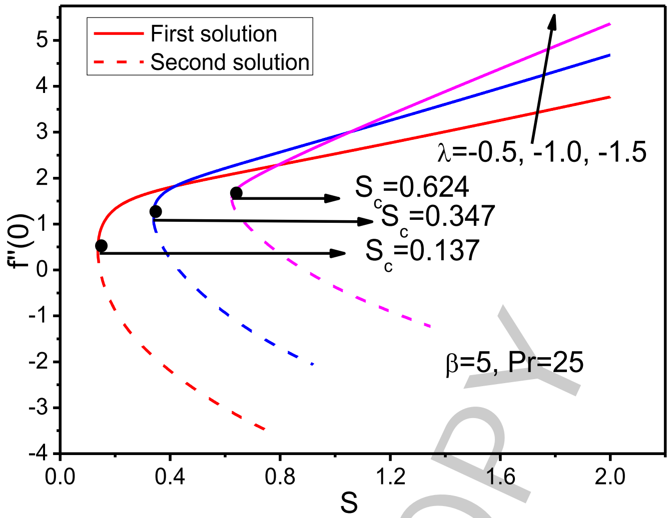

Fig. 6. Change in skin friction coefficient with change in S.

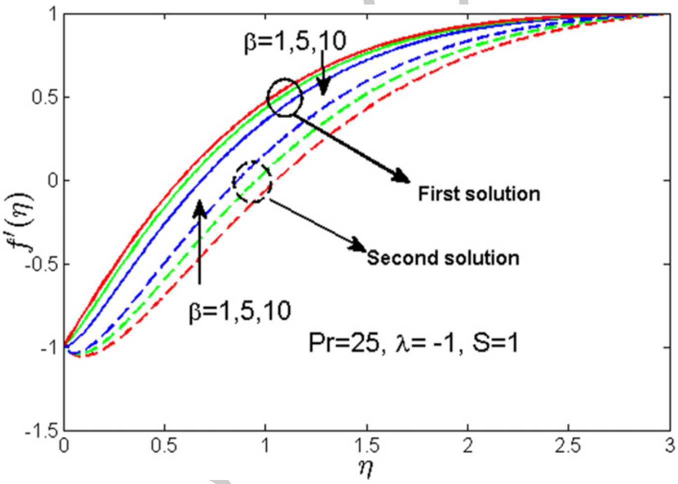

Fig. 7. Velocity profile $f'(\eta)$ for different values of β.

solutions for $0.347 < S < 0.43$ and no solution for $S < 0.347$. However, for $\beta = 10$, the solution is unique for $S > 0.44$, dual solutions for $0.372 < S < 0.44$ and no solutions for $S < 0.372$. From Fig. 5, it is seen that the critical values of the suction parameter, $S_c = 0.137, 0.347, 0.624$ for $\lambda = -0.5, -1.0, -1.5$, respectively. For $\beta = 5$, $\lambda = -1.0$, the solution is unique for $S > 1$, no solution for $S < 0.347$ and dual solutions when $0.347 < S < 1$.

An increase in the ferromagnetic parameter β results in an increase of the range of the values of the suction parameter for which the unique solution exists. Moreover, the skin friction coefficient at the surface reduces as the ferromagnetic parameter increases. On the other hand, the range of the suction parameter S for which unique solution exists is increased with an increase in the stretching parameter. Finally, the skin friction coefficient at the surface increases as the stretching parameter increases.

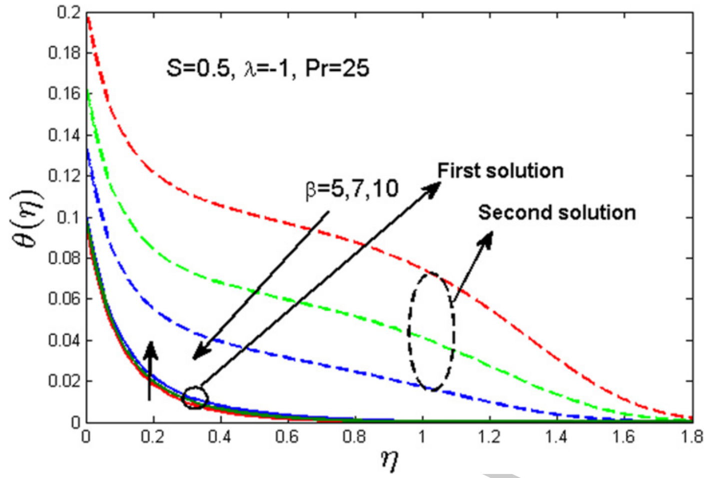

Fig. 8. Temperature profile $\theta(\eta)$ for different values of β.

Figures 7–12 depict the velocity and temperature profiles for different values of β, S, λ. Figure 7 shows that blood velocity (considered here as a biomagnetic fluid) is significantly reduced throughout the flow field as β increases, in the case of the first solution. Here β is a ferromagnetic parameter and increment of the ferromagnetic parameter results in increment of the magnetic force. This results in an increase in flow resistance. This implies that the momentum boundary layer thickness becomes thinner with a rise in the value of the parameter β. But the observation is to the contrary in the case of the second solution, for which the observation is that, an increase in the ferromagnetic parameter β results in a reduction of velocity within the boundary layer. This observation is consistent with previous studies [8,9,13]. It is apparent that the magnetic field retards the flow and that the flow resistance gives rise to an increase in temperature inside the boundary layer as well [8,9,13]. These are observed for the temperature profile of the first solution and opposite effects are observed for the second solution with increase in the ferromagnetic parameter (cf. Fig. 8). From Fig. 8 it is also observed that thermal boundary layer thickness increases for the first solution and decreases for the second solution with increase in the ferromagnetic parameter.

Figures 9 and 10 display the velocity and temperature profiles for different values of the suction parameter. Figure 9 reveals that for the first solution, the fluid velocity increases, as the suction velocity enhances, while a reverse trend is observed in the case of the second solution. This can be interpreted physically by saying that since during suction, the fluid in the vicinity of the wall is sucked away, the boundary layer thickness is reduced due to suction and thereby the fluid velocity is enhanced. Figure 10 demonstrates that the fluid temperature is reduced as the quantum of suction increases. This implies that the thermal boundary layer thickness decreases as suction proceeds. This causes an increase in the rate of heat transfer. However, this observation is valid only for the first solution. A reverse trend is found for the second solution. This observation implies that in the close vicinity of the surface, the thermal boundary layer thickness diminishes.

Figure 11 depicts the velocity profiles for different values of shrinking parameter $\lambda(<0)$. It can be noticed from this figure that by increasing the shrinking parameter, it is possible to decelerate the fluid flow significantly. This reduction in flow is caused due to the opposite directions of shrinking and free stream velocities. Figure 12 illustrates the effect of shrinking parameter λ (<0) on the temperature profiles. In this case the thermal boundary layer thickness increases as shrinking parameter increases for the first solution,

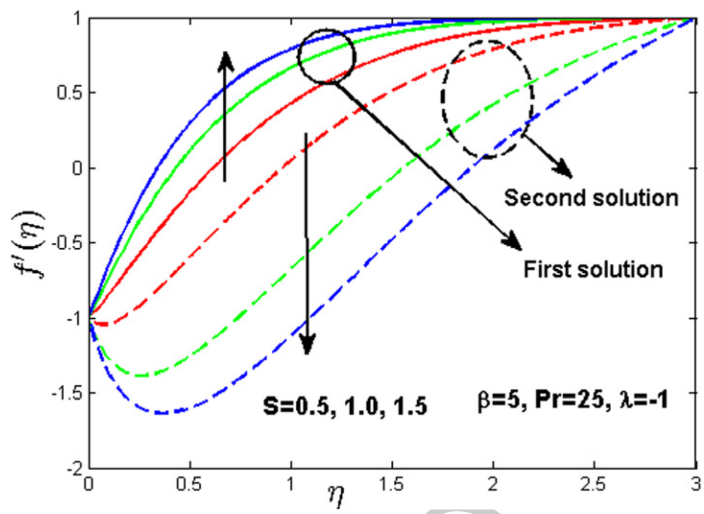

Fig. 9. Velocity profile $f'(\eta)$ for different values of S.

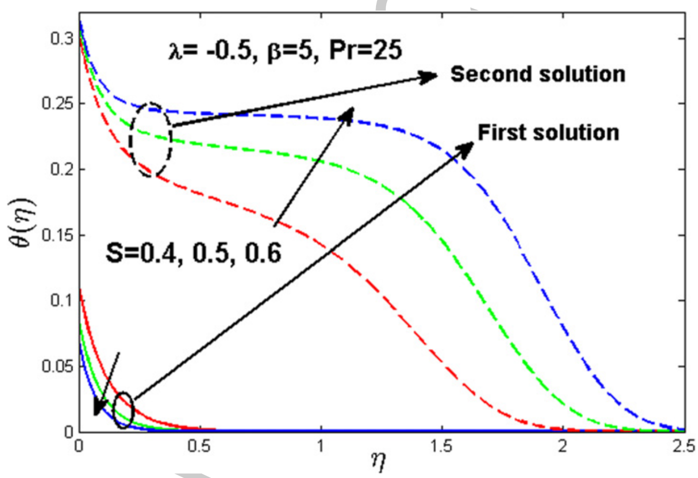

Fig. 10. Temperature profile $\theta(\eta)$ for different values of S.

but an opposite trend is observed for the second solution. Figures 7–12 also reveal that the boundary layer thickness for the second solution is always larger than that for the first solution.

6. Conclusion

This paper considered the stability of dual solutions for flow and heat transfer of biomagnetic fluids over a stretching/shrinking/ sheet in presence of a prescribed heat flux and a magnetic dipole. Numerical computation has been performed by using bvp4c function in MATLAB. Dual solutions were discussed for a certain range of stretching/shrinking parameter and suction parameter. The stability analysis reveals that the first solution is stable and physically realistic while the second solution is unstable. It can be

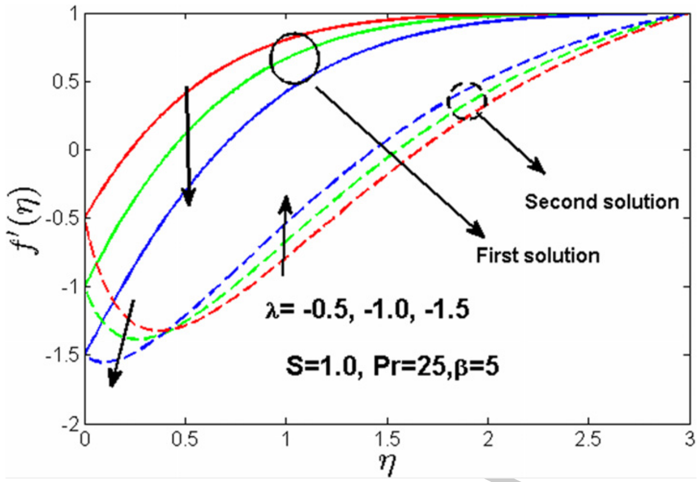

Fig. 11. Velocity profile $f^{'}(\eta)$ for different values of λ.

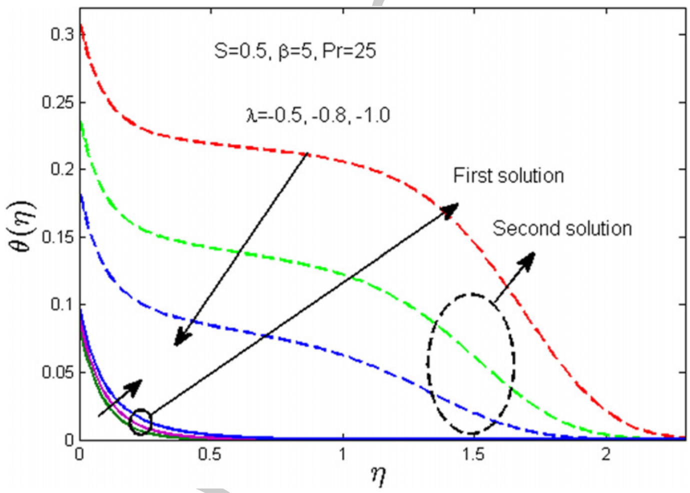

Fig. 12. Temperature profile $\theta(\eta)$ for different values of λ.

concluded from the study that the skin friction coefficient increases with an increase in the suction/stretching parameter, but it diminishes as the value of the ferromagnetic parameter increases. It can also concluded that the boundary layer thickness of both velocity and temperature for the second solution is always larger than that for the first solution.

Acknowledgements

The authors are thankful to the Reviewers for their esteemed suggestions, based on which the manuscript has been thoroughly revised.

Nomenclature

$(\boldsymbol{x}, \boldsymbol{y})$	Cartesian coordinates (m).
$(\boldsymbol{u}, \boldsymbol{v})$	Velocity components in the x, y direction $(\mathrm{m} \cdot \mathrm{s}^{-1})$.
(ξ, η)	Non-dimensional coordinates
λ	Stretching/shrinking parameter
$\overrightarrow{M}$	Magnetization $(\mathrm{A} \cdot \mathrm{m}^{-1})$
$\boldsymbol{H}$	Magnetic field intensity $(\mathrm{A} \cdot \mathrm{m}^{-1})$
$\boldsymbol{H_x}, \boldsymbol{H_y}$	Component of the magnetic field intensity $(\mathrm{A} \cdot \mathrm{m}^{-1})$
$\boldsymbol{T}$	Fluid temperature inside the boundary layer (K)
$\boldsymbol{T_c}$	Fluid temperature far away from sheet (K)
$\boldsymbol{T_w}$	Temperature of the sheet (K)
S	Suction/injection parameter
$\boldsymbol{f}'$	Dimensionless velocity component.
θ	Dimensionless Temperature
ρ	Density of fluid $(\mathrm{kg} \cdot \mathrm{m}^{-3})$
μ	Dynamic viscosity $(\mathrm{kg} \cdot \mathrm{m}^{-1}\,\mathrm{s}^{-1})$
ν	Kinematic viscosity $(\mathrm{m}^2 \cdot \mathrm{s}^{-1})$
μ_0	Magnetic permeability $(\mathrm{N} \cdot \mathrm{A}^{-2})$
$\boldsymbol{C_p}$	Specific heat constant pressure $(\mathrm{J} \cdot \mathrm{kg}^{-1}\,\mathrm{K}^{-1})$
$\boldsymbol{k}$	Thermal conductivity $(\mathrm{J} \cdot \mathrm{m}^{-1}\,\mathrm{s}^{-1}\,\mathrm{K}^{-1})$
$\boldsymbol{a}, \boldsymbol{b}$	Dimensionless constants
$\boldsymbol{P_r}$	Prandtl number (Dimensionless)
λ_a	Viscous dissipation parameter (Dimensionless)
ε	Dimensionless Curie temperature
β	Ferromagnetic interaction parameter (Dimensionless)
α	Dimensionless distance

References

[1] Y. Haik, V. Pai and C.J. Chen, Development of magnetic device for cell separation, *Journal of Magnetism and Magnetic Materials* **194** (1999), 254–261.

[2] A.N. Ruesetski and E.K. Ruuge, Magnetic fluids as drug carriers: Targeted transport of drugs by a magnetic field, *Journal of Magnetism and Magnetic Materials* **122** (1993), 335–339.

[3] M. Lauva and J. Plavins, Study of colloidal magnetite binding erythrocytes: Prospects for cell separation, *Journal of Magnetism and Magnetic Materials* **122** (1993), 349–353.

[4] J.M. Pulfer and J.K. Gallo, *Targeting Tumors Using Magnetic Drug Delivery, Biomedical Chemistry: Applying Chemical Principles to the Understanding and Treatment of Disease*, John Wiley & Sons, Inc, 2000, pp. 211–225.

[5] E.A. Gel'vich and V.N. Mazokhin, Technical aspects of electromagnetic hyperthermia in medicine, *Crit. Rev. Biomed. Eng.* **29** (2001), 77–97.

[6] Y. Haik, C.J. Chen and V. Pai, Development of biomagnetic fluid dynamics, in: *Proceedings of the IX International Symposium on Transport Properties in Thermal Fluid Engineering, Singapore, Pacific Center of Thermal Fluid Engineering*, 1996, pp. 121–126.

[7] E.E. Tzirtzilakis, A Mathematical model for blood flow in magnetic field, *Physics of Fluids* **17**(7) (2005), 077103-1-14.

[8] E.E. Tzirtzilakis and N.G. Kafoussias, Biomagnetic fluid flow over a stretching sheet with nonlinear temperature dependent magnetization, *Z. Angew. Math. Phys. (ZAMP)* **8** (2003), 54–65.

[9] E.E. Tzirtzilakis and G.B. Tanoudis, Numerical study of biomagnetic fluid flow over a stretching sheet with heat transfer, *International Journal of Numerical Methods for Heat & Fluid Flow* **13**(7) (2003), 830–848.

[10] J.C. Misra and G.C. Shit, Biomagnetic viscoelastic fluid flow over a stretching sheet, *Applied Mathematics and Computation* **210**(2) (2009), 350–361.

[11] J.C. Misra and G.C. Shit, Flow of a biomagnetic viscoelastic fluid in a channel with stretching wall, *Journal of Applied Mechanics, Trans. ASME* **76** (2009), 06106:1-9.

[12] N.A. Idris, N. Amin and H. Rahmat, Effect of gravitational acceleration on unsteady biomagnetic fluid flow, *Applied and Computational Mathematics* **3**(6) (2014), 285–294.

[13] G.M. Murtaza, E.E. Tzirtzilakis and M. Ferdows, Effect of electrical conductivity and magnetization on the biomagnetic fluid flow over a stretching sheet, *Z. Angew. Math. Phy. (ZAMP)* **68** (2017), 93.

[14] S.R.R. Reddy, P.B.A. Reddy and S. Suneetha, Magnetohydrodynamic flow of blood in a permeable inclined stretching surface with viscous dissipation, non-uniform heat source/sink and chemical reaction, *Frontiers in Heat and Mass Transfer (FHMT)* **10** (2018), 22.

[15] S. Siddiqa, S.B. Naqvi, B. Naheed, S.E. Awan and M.A. Hossain, Thermal radiation therapy of biomagnetic fluid flow in the presence of localized magnetic field, *International Journal of Thermal Sciences* **132** (2018), 457–465.

[16] S. Sushma, N. Samuel and G. Neeraja, Slip flow effects on unsteady MHD blood flow in a permeable vessel in the presence of heat source/sink and chemical reaction, *Global Journal of Pure and Applied Mathematics* **14**(8) (2018), 1083–1099.

[17] S. Mukhopadhyay, Heat transfer in a moving fluid over a moving non-isothermal flat surface, *Chin Phys. Lett.* **28**(12) (2011).

[18] K. Naganthran, R. Nazar and I. Pop, Unsteady stagnation-point flow and heat transfer of a special third grade fluid past a permeable stretching/shrinking sheet, *Scientific Reports* **6** (2016), 24632.

[19] P.M. Krishna, N. Sandeep, R. Reddy and V. Sugunamma, Dual solutions for unsteady flow of powell eyring fluid past an inclined stretching sheet, *Journal of Naval Architecture and Marine Engineering* **13** (2016), 89–99.

[20] K. Naganthran and R. Nazar, Dual solutions of MHD stagnation-point flow and heat transfer past a stretching/shrinking sheet in a porous medium, in: *4th International Conference on Mathematical Sciences AIP Conf. Proc.*, Vol. 1830, 2017, pp. 020038-1–020038-8.10.1063/1.4980901.

[21] E.H. Hafidzuddin, R. Nazar, N.M. Arifin and I. Pop, Boundary layer flow and heat transfer over s permeable exponentially stretching/shrinking sheet with generalized slip velocity, *Journal of Applied Fluid Mechanics* **9**(4) (2016), 2025–2036.

[22] S. Ghosh, S. Mukhopadhyay and K. Vajravelu, Dual solutions of slip flow past a nonlinearly shrinking permeable sheet, *Alexandria Engineering Journal* **55**(2) (2016), 1835–1840.

[23] M.H.M. Yasin, A. Ishak and I. Pop, MHD heat and mass transfer flow over a permeable stretching/shrinking sheet with radiation effect, *Journal of Magnetism and Magnetic Materials* **407** (2016), 235–240.

[24] I.S. Awaludin, P.D. Weidman and A. Ishak, Stability analysis of stagnation-point flow over a stretching/shrinking sheet, *AIP Advances* **6** (2016), 0453081-7.

[25] U. Mishra and G. Singh, Dual solutions of mixed convection flow with momentum and thermal slip flow over a permeable shrinking cylinder, *Computers & Fluids* **93** (2014), 107–115.

[26] K. Bhattacharyya, Dual solutions in unsteady stagnation-point flow over a shrinking sheet, *Chin Phys. Lett.* **28**(8) (2011), 084702.

[27] T. Hayat, M. Imtiaz and A. Alsaedi, Partial slip effects in flow over nonlinear stretching surface, *Applied Mathematics and Mechanics (Engl. Ed.)* **36**(11) (2015), 1513–1526.

[28] M. Bovand, S. Rashidi and J.A. Esfahani, Optimum interaction between magnetohydrodynamics and nanofluid for thermal and drag management, *Journal of Thermophys. Heat Transfer* **31** (2016), 218–229.

[29] S. Das, S. Chakraborty, R.N. Jana and O.D. Makinde, Entropy analysis of unsteady magneto-nanofluid flow past accelerating stretching sheet with convective boundary condition, *Applied Mathematics and Mechanics (Engl. Ed.)* **36**(12) (2015), 1593–1610.

[30] S. Rashidi, M. Bovand and J.A. Esfahani, Structural optimization of nanofluid flow around an equilateral triangular obstacle, *Energy* **88** (2015), 385–398.

[31] S. Rashidi, M. Bovand and J.A. Esfahani, Opposition of magnetohydrodynamic and Al_2O_3-water nanofluid flow around a vertex facing triangular obstacle, *Journal of Molecular Liquids* **215** (2016), 276–284.

[32] S.Z. Shirejini, S. Rashidi and J.A. Esfahani, Recovery of drop in heat transfer rate for a roating system by nanofluids, *Journal of Molecular Liquids* **220** (2016), 961–969.

[33] S. Aktar, S. Rashidi and J.A. Esfahani, Second law of thermodynamic analysis of nano fluid turbulent flow around a rotating cylinder, *Journal of Thermal Analysis and Calorimetry* **132** (2018), 1189–1200.

[34] S. Rashidi, J.A. Esfahani and M. Maskaniyan, Applications of magnetohydrodynamics in biological systems-A review on the numerical studies, *Journal of Magnetism and Magnetic Materials* **439** (2017), 358–372.

[35] T. Hayat, A. Shafiq, A. Alsaedi and S.A. Shahzad, Unsteady MHD flow over exponentially stretching sheet with slip conditions, *Applied Mathematics and Mechanics (Engl. Ed.)* **37**(2) (2016), 193–208.

[36] F.M. Ali, R. Nazar, N.M. Arifin and I. Pop, MHD stagnation-point flow and heat transfer towards stretching sheet with induced magnetic field, *Applied Mathematics and Mechanics (Engl. Ed.)* **32**(4) (2011), 409–418.

[37] B. Ahmed, Z. Iqbal and E. Azhar, Combined effects of internal heat generation and mass effects on MHD Casson fluid with convective boundary conditions, *International Journal of Applied Electromagnetics and Mechanics* **54**(2) (2017), 1–11.

[38] J.M. Jalil and K.A. Al-Tae'y, Natural convection in an enclosure under the influence of time-periodic magnetic field, *International Journal of Applied Electromagnetics and Mechanics* **31** (2009), 97–111.

[39] Z. Wang, C. Liu and W. Wei, Industry applications of magnetic separation based on nanoparticles: A review, *International Journal of Applied Electromagnetics and Mechanics* **1** (2019), 1–17.

[40] M. Bovand, S. Rashidi, J.A. Esfahani and R. Masoodi, Control of wake destructive behavior for different bluff bodies in channel flow by magnetohydrodynamics, *Eur. Phys. J. Plus* **131** (2016), 194.

[41] S. Rashidi and J.A. Esfahani, The effect of magnetic field on instabilities of heat transfer from an obstacle in a channel, *Journal of Magnetism and Magnetic Materials* **391** (2015), 5–11.

[42] S. Rashidi, M. Bovand and J.A. Esfahani, Application of magnetohydrodynamics for suppressing the fluctuations in the unsteady flow around two side-by-side circular obstacles, *Eur. Phys. J. Plus* **131** (2016), 423.

[43] K. Naganthran, R. Nazar and I. Pop, Unsteady stagnation-point flow and heat transfer of a special third grade fluid past a permeable stretching/shrinking sheet, *Scientific Reports* **6** (2016), 24632.

[44] A. Majeed, A. Zeeshan and R. Ellahi, Unsteady ferromagnetic liquid flow and heat transfer analysis over a stretching sheet with the effect of dipole and prescribed heat flux, *Journal of Molecular Liquids* **223** (2016), 528–533.

[45] L.S. Titus and A. Abraham, Ferromagnetic liquid flow due to gravity-aligned stretching of an elastic sheet, *Journal of Applied Fluid Mechanics* **8**(3) (2015), 591–600.

[46] J.C. Misra, B. Mallick and P. Steinmann, Temperature distribution and entropy generation during Darcy–Forchheimer–Brinkman electrokinetic flow in a microfluidic tube subject to a prescribed heat flux, *Meccanica* **55** (2020), 1079–1098.

[47] S. D Harris, D. B Ingham and I. Pop, Mixed convection Boundary-layer flow near the stagnation point on a vertical surface in a porous medium: Brinkman model with slip, *Transp. Porous Media* **77** (2009), 267-285.